Geometry of the edge of chaos in a low-dimensional turbulent shear flow model

Madhura Joglekar,[1] Ulrike Feudel,[2] and James A. Yorke[1]
[1]*University of Maryland, College Park, Maryland 20742, USA*
[2]*Theoretical Physics/Complex Systems, ICBM, Carl von Ossietzky University Oldenburg, PF 2503, D-26111 Oldenburg, Germany*
(Received 31 August 2014; published 7 May 2015)

We investigate the geometry of the edge of chaos for a nine-dimensional sinusoidal shear flow model and show how the shape of the edge of chaos changes with increasing Reynolds number. Furthermore, we numerically compute the scaling of the minimum perturbation required to drive the laminar attracting state into the turbulent region. We find this minimum perturbation to scale with the Reynolds number as Re^{-2}.

DOI: 10.1103/PhysRevE.91.052903 PACS number(s): 05.45.Pq, 47.52.+j

I. INTRODUCTION

Understanding the transition to turbulence is a long-lasting problem in fluid dynamics, particularly in the case of simple flows in which the base flow does not become linearly unstable. This applies to the Hagen-Poiseuille or pipe flow, which is stable for all Reynolds numbers Re, or the plane Couette flow [1].

At low Reynolds numbers, all initial conditions decay to the laminar profile for those flows. At higher Reynolds numbers, above a critical value, perturbations of the flow obtained by, e.g., placing obstacles into the flow or making boundaries of the pipe or the plates rough enough can lead to turbulent states, which may last for a long time. As the Reynolds number increases, smaller perturbations are required to destabilize the laminar flow. The magnitude of the perturbation that disrupts the laminar flow depends not only on the Reynolds number, but also on the direction of the perturbation. Here direction refers to direction in infinite-dimensional state space. Thus, some directions require a much larger magnitude perturbation to destabilize the laminar flow to turbulent states, as compared to others. Low-dimensional models, based on the Galerkin method, have been used to better understand the turbulent behavior [2–7]. Depending on the model and the Reynolds number, when the system exhibits turbulence, the turbulent state can be either transient or sustained. Here we continue the practice of referring to transient or sustained chaotic oscillations obtained in low-dimensional models as turbulence [2–7]. Low-dimensional models can be suggestive of properties observed in higher-dimensional models. For example, the nine-dimensional model in [8] suggested ideas which were followed up in the ≈120 000-dimensional model [9], which turned out to have similar properties. However, there are no guarantees that low-dimensional phenomena will be reflected in the higher-dimensional model.

Numerical simulations and experiments for plane Couette flow [7,10–12] and pipe flow [10,13–18] show that the turbulent state is transient for lower Reynolds numbers. In the transient turbulence region, the system exhibits an exponential distribution of lifetimes (where the *lifetime* is the time taken for a given trajectory to reach a specified distance from the laminar attractor). This exponential distribution is indicative of a chaotic saddle (nonattracting chaotic invariant set). A transition of turbulence from transient to sustained, i.e., from a chaotic saddle to a chaotic attractor, would require a boundary crisis [19] and would result in a diverging average lifetime of a trajectory. References [10–18] show that the median lifetime varies as $1/(\mathrm{Re}_c - \mathrm{Re})$, where Re_c denotes the critical Reynolds number, beyond which the system exhibits sustained turbulence coexisting with the laminar attracting state; that is, the turbulent state is a chaotic attractor. Other studies [2,20,21] suggest that the average lifetime of a trajectory increases rapidly with Reynolds number, but does not diverge, and present evidence that it increases exponentially, so that the turbulent state is transient for all Reynolds numbers. Hof *et al.* [22] have shown for the pipe flow that no critical point for the transition to persistent turbulence exists. More recently, experiments and extensive numerical simulations have revealed that there is a transition between the laminar and the turbulent state for higher Reynolds numbers ($\mathrm{Re} > 2300$) [23,24]. Moreover, the trajectories for high Reynolds numbers possess a memory expressed by a superexponential scaling with the Reynolds number. The explanation of this transition is based on the existence of spatially localized turbulent structures, so-called puffs, which become more frequent at higher Reynolds numbers. This finding suggests not only that the transition to turbulence is due to a more complex temporal structure of the flow field, but that spatial aspects need to be taken into account.

Recognizing the great difficulty of conducting such studies for the full partial differential equations for the fluid flow, we examine, instead, a nine-dimensional model of sinusoidal shear flow [2,25,26] that is a generalization of the model in [27]. In this model, since the laminar state is linearly stable, irrespective of whether the turbulent state is a chaotic saddle or a chaotic attractor, infinitesimal perturbations applied to the laminar state will always decay. Evidence of the one or the other scenario can only be obtained using finite size perturbations. While transient turbulent states are related to finite though possibly very long decay times, permanent turbulence will be reached by perturbations which never decay.

Choosing any initial condition lying in the basin of the laminar attractor, and moving along any direction in the nine-dimensional space, one almost always encounters turbulent behavior, and this turbulent behavior is preceded by a discontinuity in the lifetimes. Such a point of discontinuity is said to lie in the "edge of chaos" [8]. The first computation of the edge in a pipe flow has been reported in [28]. Lebowitz [29,30] examines the emergence of the edge via a homoclinic bifurcation and its stability behavior in low-dimensional models of a shear flow. Lebowitz *et al.* [31] analyze the structure of the edge in low-dimensional shear flow models and show that the

edge winds endlessly around the orbits which decay more slowly towards the laminar state, so that the slow-decaying orbits can circumnavigate the edge to reach the laminar state. Reference [32] studies the structure of the edge in a numerical model of the plane Couette flow with $64 \times 36 \times 64$ modes.

Reference [33] investigates the structure of the stable manifold of the saddle on the edge for the plane Couette flow, based on minimal-energy perturbations to the laminar state that reach the edge, using time as a parameter. Reference [34] investigates a plane Couette flow and uses an optimization method to compute the minimal-energy perturbations inducing transition, as a combination of a finite number of linear optimal modes. More recently, a variational method [35] has been used to investigate the nonlinear stability of the pipe flow [36,37] and the plane Couette flow [38–41]. This method determines "the minimal seed of turbulent transition [37]," that is, the initial condition of minimal energy leading eventually to the edge state by optimizing a functional linked to turbulence, such as the perturbation kinetic energy [36,37,39,40] or the time-averaged dissipation [38,41] over all possible initial disturbances of a given magnitude. These initial disturbances evolve based on the Navier-Stokes equations to a large target time. The initial disturbance norm is gradually increased until a sudden jump is observed in the optimized functional. The jump corresponds to encountering a state lying beyond the edge. Different exponents relating the scaling of the critical amplitude with respect to the Reynolds number have been computed using different numerical models [3,9,42–44]. Experiments for the pipe flow conducted in different laboratories yield exponents which partly differ [45–47].

While the particular notion of the edge is slightly different depending on whether turbulence is transient or sustained, its procedure of identification is very similar. The edge denotes the accessible part of the boundary, where a path in a basin might terminate. Most points of a fractal boundary are surrounded by infinitely many layers of boundary and these are not in the edge. In case of a transient turbulent state, the edge denotes the "boundary" of the chaotic saddle which is embedded in the basin of attraction of the laminar state and is accessible from that state. In case of bistability with the coexistence of a laminar and a turbulent state, the edge is considered to be the boundary of the basin of attraction. This boundary has been shown to be the stable manifold of a periodic saddle or of a chaotic saddle embedded in the basin boundary [7,9,26]. The distance of the edge of chaos from the laminar attractor indicates the *minimum perturbation* that would destabilize the laminar attracting state. This is referred to as the *critical amplitude*.

Here we address the Reynolds number dependence of the minimum perturbation required to drive the laminar attracting state into the turbulent region regardless of whether transient or sustained turbulence occurs. For this purpose we employ the nine-dimensional sinusoidal shear flow model studied in [2,25,26]. This minimum perturbation is closely related to the edge of chaos introduced in [8]. Our goal is to gain greater understanding of the geometry of the edge of chaos, particularly emphasizing those edge of chaos points that are closest to the laminar attractor and hence correspond to those directions, which start from the laminar attractor and require relatively small perturbations to create transient chaos. We examine the geometry of the edge of chaos to see how the distance of the edge from the laminar attractor, and consequently "the stability of the laminar attractor," varies as a function of the Reynolds number.

Section II starts with a brief description of the model; then we discuss some basic definitions (Sec. III), along with the method to follow along the edge of chaos in a high-dimensional phase space. In Sec. IV, we compute the minimal perturbation needed to reach the edge of chaos and, hence, to drive the system to a turbulent state, which is either transient or permanent, depending on the Reynolds number. Additionally, we discuss the nontrivial attracting orbits and the structure of their basins of attraction. Furthermore, in Sec. V, we discuss our results related to the dependence of lifetimes and the geometry of the edge on Reynolds number and compare them with previous findings.

II. THE MODEL OF THE SINUSOIDAL SHEAR FLOW

For the purpose of our study, we investigate the nine-dimensional sinusoidal shear flow model examined in [2,25,26].

In the model, the fluid between two free-slip walls experiences a sinusoidal body force. The coordinate system is such that x points downstream, y in the direction of the shear, and z in the spanwise direction. d is the distance between the walls, ρ is the fluid density, and ν is the kinematic viscosity. The characteristic velocity U_0 is the laminar velocity that arises due to the forcing at a distance $d/4$ from the top wall. The Reynolds number is defined as $\mathrm{Re} = \frac{U_0 d}{2\nu}$. The lengths are nondimensionalized in units of $d/2$, velocities in units of U_0, time in units of $(d/2)/U_0$, and pressure in units of $\rho {U_0}^2$. Then the evolution equation is

$$\frac{\partial u}{\partial t} = -(u \cdot \nabla)u - \nabla p + \frac{\nabla^2 u}{\mathrm{Re}} + F(y).$$

As the fluid is incompressible, $\nabla \cdot u = 0$. There are free-slip boundary conditions at the walls at $y = \pm 1$; hence,

$$u_y|_{y=\pm 1} = 0, \quad \left.\frac{\partial u_x}{\partial y}\right|_{y=\pm 1} = \left.\frac{\partial u_z}{\partial y}\right|_{y=\pm 1} = 0.$$

It is assumed that the flow is periodic in the streamwise and spanwise directions, with lengths L_x and L_z, respectively. References [2,25,26] analyze the flow for a domain with $L_x = 4\pi, L_z = 2\pi$ (which corresponds to the optimal domain size for a plane Couette flow to obtain the formation of stationary coherent structures), as well as for a narrower domain with $L_x = 1.75\pi, L_z = 1.2\pi$ (which corresponds to the minimum domain size that can sustain turbulence for plane Couette flow). We focus on the latter case $L_x = 1.75\pi, L_z = 1.2\pi$.

The nondimensionalized volume force is

$$F(y) = \frac{\sqrt{2}\pi^2}{4\mathrm{Re}} \sin(\pi y/2)\hat{e}_x.$$

The full model is given in the Supplemental Material [48], and a detailed discussion of the modes and their interaction is given in [2]. We write the state of the model as

$$a(t) = (a_1(t), \ldots, a_9(t)),$$

where $a_i(t), i = 1,2,\ldots,9$ are the time-dependent coefficients that multiply the different spatial modes. The laminar state of the model, which is linearly stable for all Reynolds numbers, corresponds to a fixed point,

$$a_1 = 1, \quad a_2 = a_3 = \cdots = a_9 = 0.$$

As in [26], which studies the same model we do, the fluctuation energy with respect to the laminar profile is defined as $E = (1 - a_1)^2 + \sum_{j=2}^{9} {a_j}^2$. Thus, each initial condition $a(0)$ for the nine-dimensional model can be associated to the initial energy of the perturbation. For Re < 335 and $515 <$ Re < 1000, the laminar state is the only attractor in the system, while the turbulent state is transient and represents a chaotic saddle. For $335 <$ Re < 515, the system has a symmetric pair of stable "nontrivial" attractors associated with sustained turbulence, besides the laminar attractor.

III. THE EDGE OF CHAOS

Let us first give some definitions related to our study.

Lifetime. The lifetime associated to a given point is defined as the time it takes for the trajectory starting from a point to reach a specified distance from the laminar attractor. This specified distance is implemented as a small ball around the fixed point corresponding to the laminar state.

The edge of chaos. As one travels along a direction through state space, starting from any point in the basin of the laminar attractor, the edge is the locus of the first point which is encountered where the lifetime goes to infinity.

Although the lifetime approaches infinity along the edge, the turbulent region beyond the edge is unstable for a large interval of Reynolds numbers, and hence has finite, though possibly very long, lifetimes. The edge of chaos is a measure 0 set, and hence it is numerically impossible to encounter the points along the edge with arbitrarily large lifetimes. Within the interval of Reynolds numbers where also the pair of symmetric nontrivial attractors coexist with the stable laminar state, the lifetimes are as large as the integration time, when a trajectory is in the basin of attraction of one of the nontrivial attractors.

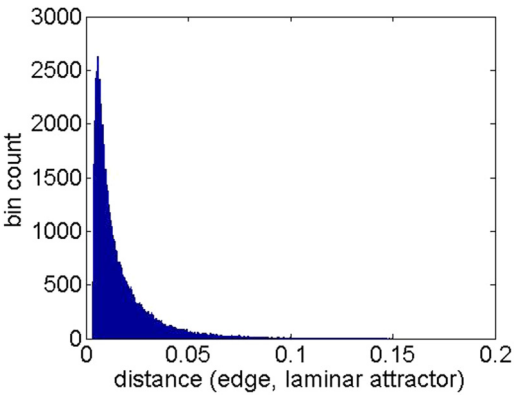

FIG. 1. (Color online) The histogram shows the distance of the edge from the laminar attractor for 100 000 randomly chosen directions in the nine-dimensional state space, at Re = 400. The bin size is 0.0003. The largest bin count of 2620 is at the bin centered at 0.005 76.

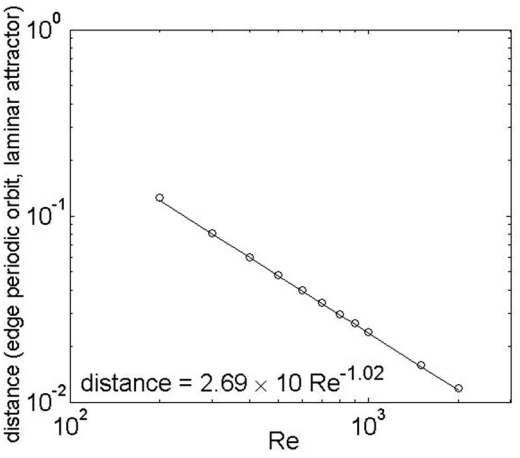

FIG. 2. The distance of the periodic orbit on the edge from the laminar attractor on the y axis vs Reynolds number on the x axis is plotted, for Re = 200, 300, . . . , 1000, 1500, 2000.

In Fig. 1, the histogram plots the distance of the edge from the laminar attractor for 100 000 randomly chosen directions in the nine-dimensional state space at Re = 400.

Following the edge of chaos. To *follow* along the edge of chaos, we use the technique outlined in [49]. Choosing a direction from the laminar attractor towards the edge, an initial condition on the path before the edge point is reached, gives a trajectory whose amplitude remains small as it relaxes to the laminar state. Conversely, an initial condition chosen beyond the edge generates a trajectory with a chaotic transient typically containing at least one large amplitude excursion before decaying. Repeated bisection can be used to reduce the distance between the two initial conditions to obtain a new pair of points that approximate the edge point. Trajectories starting from this new pair of points are then followed until the distance between them exceeds a given threshold, followed by bisection and so on, thus producing a numerical approximation to an edge trajectory.

We follow along the edge trajectory starting from a randomly chosen direction, for Reynolds numbers from 200 to 2000. Our computations indicate that in each case, the trajectory converges to a periodic orbit on the edge. In Fig. 2, the distance of the periodic orbit on the edge from the laminar attractor, is plotted as a function of Reynolds number, for Re $= 200,300,\ldots,1000,1500,2000$. The distance of the periodic orbit from the laminar attractor scales as $\approx$Re^{-1} (see Fig. 2).

IV. THE GEOMETRY OF THE EDGE OF CHAOS

A. Contour graphs for three orthogonal vectors

To examine the edge of chaos, we choose three mutually orthogonal vectors starting from the laminar attractor, namely, $v1 = [1,1,1,1,1,1,1,1,1]$, $v2 = [-1,1,2,0,1,0,-1,0,-2]$, and $v3 = [1,-1,0,1,0,-1,-2,2,0]$. We look at two different planes: plane 1, formed by vectors $v1$ and $v2$, and plane 2, formed by vectors $v1$ and $v3$. Figures 3(a), 3(c), and 3(e) show the contour plots for the lifetimes in plane 1, for Reynolds numbers 200, 400, and 1000, respectively. Figures 3(b), 3(d),

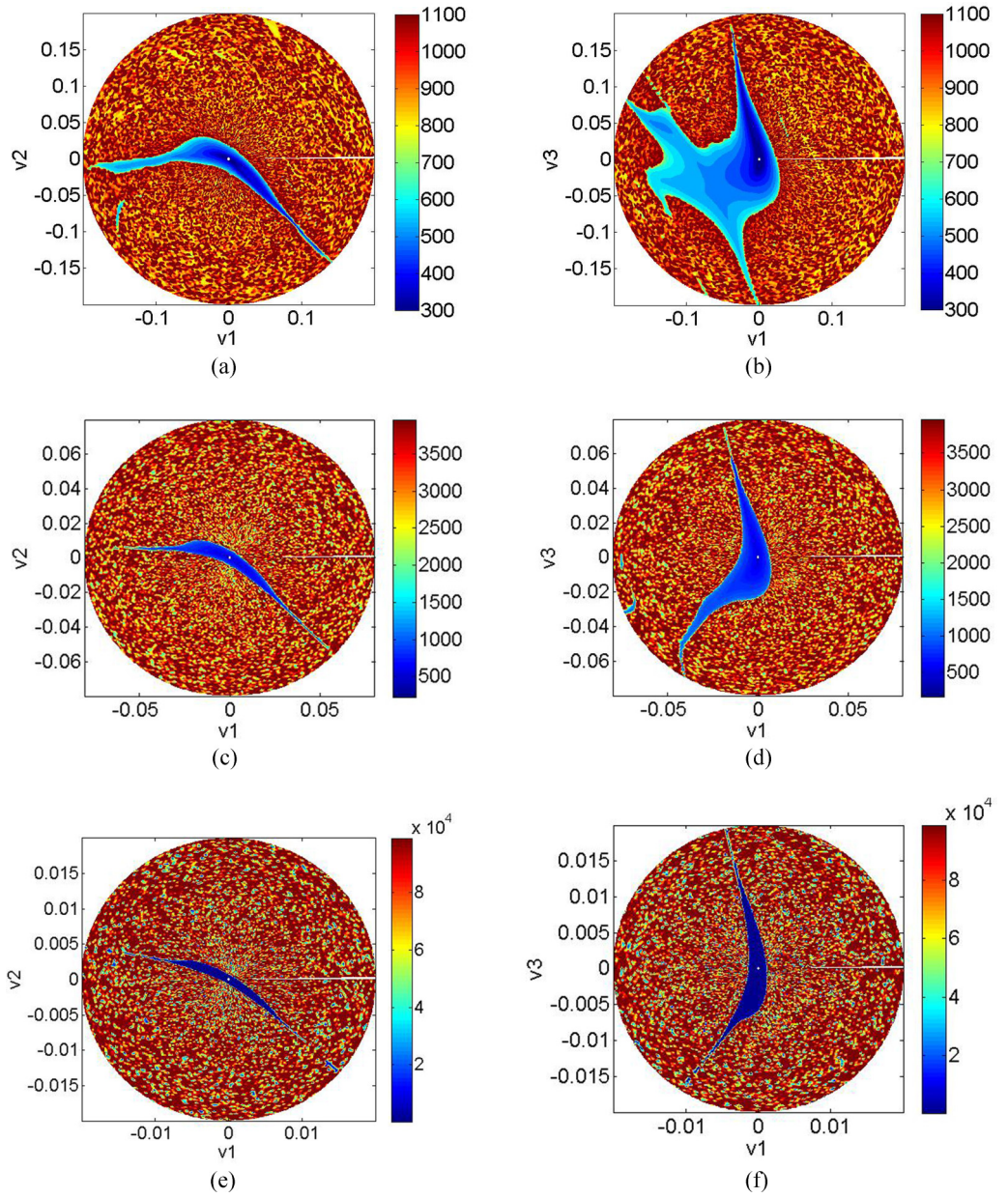

FIG. 3. (Color online) Panels (a), (c), and (e) show the contour plots for the lifetimes, in the plane 1 formed using orthogonal vectors $v1$ and $v2$, for Reynolds numbers 200, 400, and 1000, respectively. Panels (b), (d), and (f) show the contour plots for the lifetimes, in the plane 2, formed using orthogonal vectors $v1$ and $v3$, for Reynolds numbers 200, 400, and 1000, respectively. In each of the plots, the points with lifetimes exceeding the maximum value indicated by the color bar are color coded with the color corresponding to the maximum value. The figure is shifted so that the origin corresponds to the laminar attractor.

and 3(f) show the contour plots for the lifetimes in plane 2, for Reynolds numbers 200, 400, and 1000, respectively. The figure is shifted so that the origin corresponds to the laminar attractor. In each of the plots, the points with lifetimes exceeding the maximum value indicated by the color bar are color coded with the color corresponding to the maximum value.

B. Lifetime distribution

For $335 < \mathrm{Re} < 515$, the system has a symmetric pair of stable "nontrivial" attractors, besides the laminar attractor. For $\mathrm{Re} < 335$ and $515 < \mathrm{Re} < 1000$, the laminar state is the only attractor. Reference [2] observes an exponential distribution of lifetimes for those values of Reynolds number for which the laminar attractor is the only attractor, indicative of the turbulent state being a chaotic saddle. This was also observed by us. This exponential distribution can be used to compute the average lifetime τ of the transients at those Reynolds numbers for which the laminar attractor is the only attracting state. Hence, we use $\mathrm{Re} =$ 200, 300, 600, 700, 800, 900, 1000, 1500, 2000 to study the distribution of the average lifetimes. In Fig. 4, $1/\tau$ is plotted as a function of the Reynolds number, where τ denotes the average lifetime. The figure indicates that $\tau \sim \mathrm{Re}^{4.51}$.

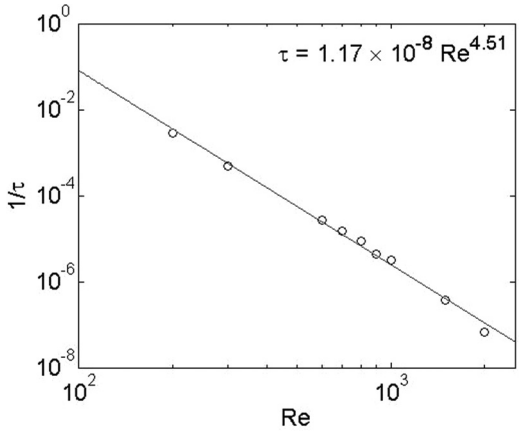

FIG. 4. $1/\tau$ vs Re is plotted for Re = 200, 300, 600, 700, 800, 900, 1000, 1500, 2000. Here τ is the average lifetime. Note that we exclude Re = 400, 500. Because of the presence of a nontrivial attractor at Re = 400, 500 (sustained turbulence instead of transient turbulence corresponding to a chaotic saddle), the average lifetime for convergence to the laminar attractor is not defined.

Let us now illustrate the dependence of the lifetimes on the distance of the initial state from the laminar state. For Re = 600, we compute the lifetimes for points in plane 1 starting from the laminar attractor until radius values of 0.05 [similar to Figs. 3(a), 3(c), and 3(e)]. We observe that points that lie within the edge with trajectories converging quickly to the laminar attractor have lifetimes <2900, and a sudden jump in lifetimes is observed for points lying on the other side of the edge, which exhibit turbulent behavior before reaching the laminar attractor. For points having lifetimes exceeding 2900, Fig. 5 plots the radial distance on the x axis vs lifetime on the y axis. Observe that in this transient turbulence region, the distribution of lifetimes is largely independent of radial distance.

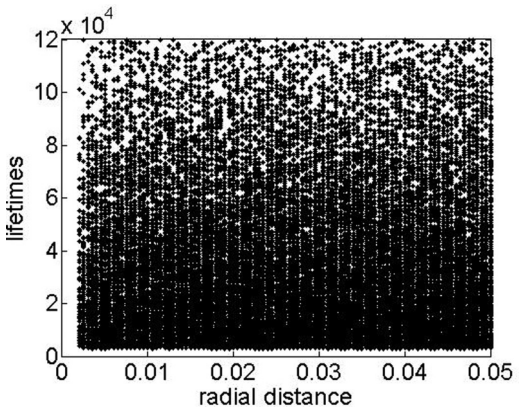

FIG. 5. For Re 600, we compute the lifetimes for points in plane 1 starting from the laminar attractor until radius values of 0.05. The figure considers those points lying in the turbulent region and plots the corresponding radial distance on the x axis vs lifetime on the y axis. Observe that in the transient turbulence region, the distribution of lifetimes is largely independent of radial distance.

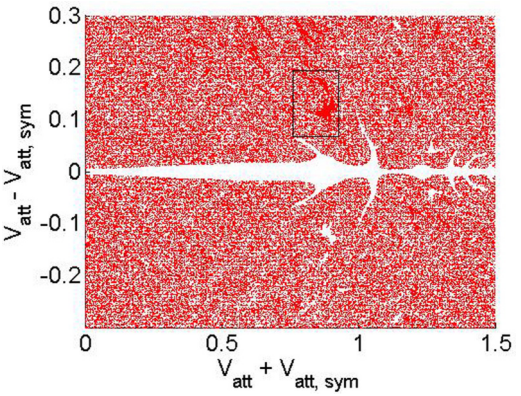

FIG. 6. (Color online) The basin of attraction corresponding to P_{att} is plotted in red (dark gray), where $P_{\text{att}} \approx (0.877, 0.115)$. The black rectangle denotes the region which is magnified in Fig. 7.

C. Nontrivial attracting orbits

The system has a symmetric pair of nontrivial attractors associated with sustained turbulence, apart from the laminar attractor, for $335 < \text{Re} < 515$. The nontrivial attractors can be periodic, chaotic, or quasiperiodic. We investigate the pair of attractors at Re = 425, where the attractors are periodic. For this, we choose a point on one of the nontrivial attracting orbits (we call this point P_{att}) and the corresponding point on the symmetric attracting orbit (we call this point $P_{\text{att,sym}}$).

We choose P_{att} such that $a_1 = 0.129\,992, a_2 = -0.065\,592\,9$, $a_3 = 0.047\,570\,6$, $a_4 = 0.032\,996\,7$, $a_5 = 0.075\,385\,4$, $a_6 = -0.003\,250\,98$, $a_7 = -0.042\,364$, $a_8 = -0.019\,685, a_9 = -0.101\,453$, so that for $P_{\text{att,sym}}$, $a_1 = 0.129992$, $a_2 = 0.065\,592\,9$, $a_3 = -0.047\,570\,6$, $a_4 = -0.032\,996\,7$, $a_5 = -0.075\,385\,4$, $a_6 = -0.003\,250\,98$, $a_7 = -0.042\,364, a_8 = -0.019\,685, a_9 = -0.101\,453$. We look at a plane containing the laminar attractor and the points P_{att} and $P_{\text{att,sym}}$. Say the vector directed from the laminar attractor to P_{att} is called V_{att} and the vector directed from the laminar attractor to $P_{\text{att,sym}}$ is called $V_{\text{att,sym}}$. Then the vectors $V_{\text{att}} + V_{\text{att,sym}}$ and $V_{\text{att}} - V_{\text{att,sym}}$ are orthogonal. In Figs. 6 and 7, the x axis is along $V_{\text{att}} + V_{\text{att,sym}}$ and the y axis is along $V_{\text{att}} - V_{\text{att,sym}}$.

The figures are shifted so that the origin corresponds to the laminar attractor. The x and y coordinates corresponding to P_{att} in the x-y plane are $\approx(0.877, 0.115)$ and the coordinates corresponding to $P_{\text{att,sym}}$ are $\approx(0.877, -0.115)$. In this plane, Fig. 6 shows the basin of attraction corresponding to P_{att} in red (dark gray) for $x \in [0, 1.5], y \in [-0.3, 0.3]$. In Figs. 7(a)–7(c) we magnify the region close to P_{att} denoted by the black rectangle in Fig. 6. Figure 7(a) shows the basin of attraction corresponding to P_{att} in red (dark grey). Figure 7(b) shows the basin of attraction corresponding to $P_{\text{att,sym}}$ in black. Figure 7(c) shows the basin of attraction corresponding to the laminar attractor in blue (dark gray). We can see from Fig. 7(a) that the open neighborhood around P_{att} containing only points lying in the basin of attraction corresponding to P_{att} is small. Most of the state space is filled with transient chaos and the basins of attraction of the attractors are well mixed. Eckhardt and co-workers [50,51] study the bifurcations of the nontrivial attracting orbits in the plane Couette flow, using

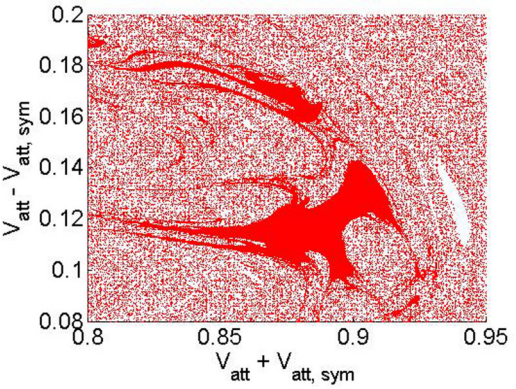

(a)

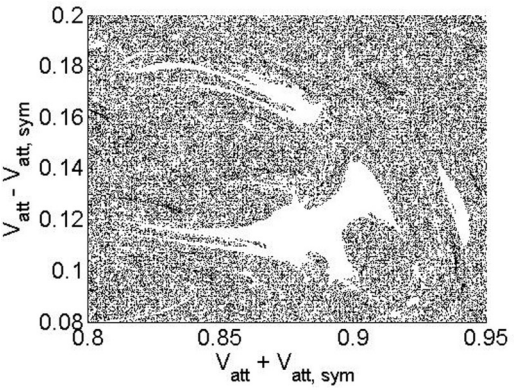

(b)

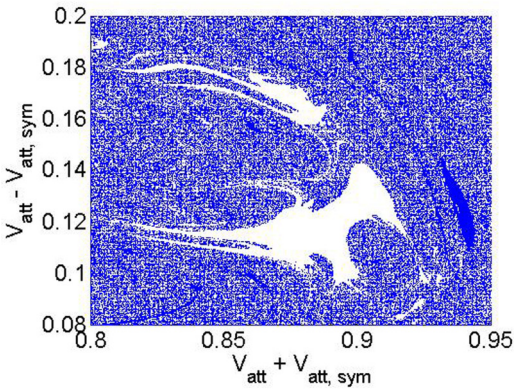

(c)

FIG. 7. (Color online) Panels (a), (b), and (c) are magnifications of the black rectangle shown in Fig. 6, close to P_{att} and plot the basins of attraction corresponding to P_{att} in red (dark gray), to P_{attsym} in black, and to the laminar attractor in blue (dark gray), respectively.

a numerical resolution of $32 \times 33 \times 32$ and $48 \times 33 \times 48$ modes, respectively. Their papers contain basin of attraction plots similar to Fig. 7(a), which seems to suggest an analogous behavior in full high-dimensional flows.

D. Properties of the edge as a function of Reynolds number

According to the aim of this study, we now present our results on the minimum perturbation necessary to destabilize the laminar state. To this end, we choose 10 000 directions randomly in the nine-dimensional state space,

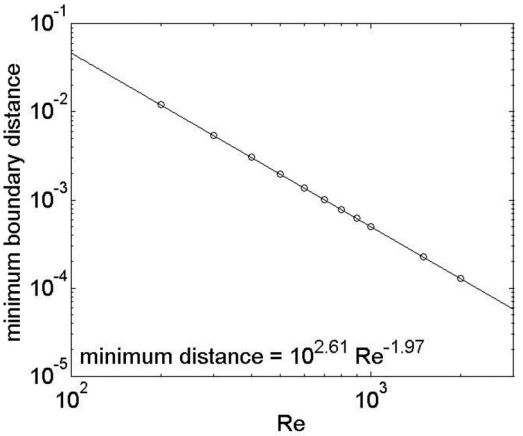

FIG. 8. For 10 000 randomly chosen vectors, the minimum distance from the edge of chaos vs Reynolds number is plotted for Re = 200, 300, ..., 1000, 1500, 2000.

starting from the laminar attractor. For these directions, we compute the minimum, the average, and the maximum distance from the edge of chaos, respectively, and plot them as a function of the Reynolds number, for Re = 200, 300, ..., 1000, 1500, 2000 in Figs. 8–10. Of particular interest is the minimum distance since it corresponds to the minimum perturbation necessary to destabilize the laminar state leading to a transient or sustained turbulent motion. The obtained scaling with the Reynolds number is $\sim Re^{-2}$.

V. DISCUSSION

We have studied a nine-dimensional model of the sinusoidal shear flow to contribute to a greater understanding of the geometry of the edge of chaos playing a crucial role in the transition from a laminar state to transient or sustained turbulence. In this low-dimensional model the transient or sustained turbulent state correspond to either a chaotic saddle or a chaotic attractor, respectively. Of particular interest are such finite-size perturbations which destabilize the laminar state. The latter is for the whole considered interval of Reynolds numbers linearly

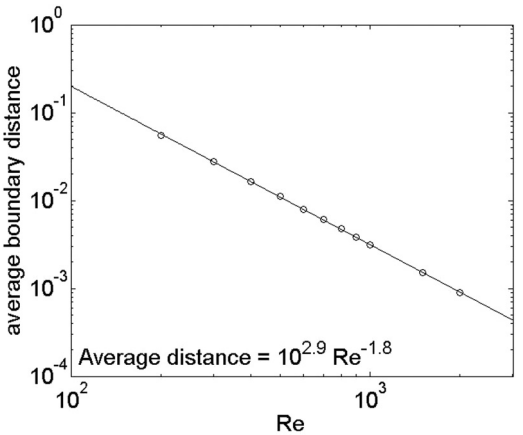

FIG. 9. For 10 000 randomly chosen vectors, the average distance from the edge of chaos vs Reynolds number is plotted, for Re = 200, 300, ..., 1000, 1500, 2000.

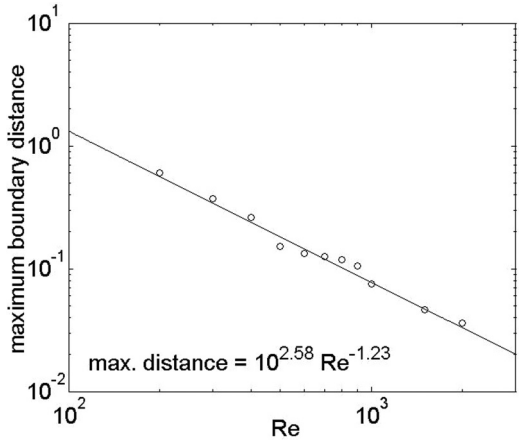

FIG. 10. For 10 000 randomly chosen vectors, the maximum distance from the edge of chaos vs Reynolds number is plotted, for Re = 200, 300, . . . , 1000, 1500, 2000. We believe that the deviation from the scaling of the maximum boundary distance is caused by the bending of the long tendril-like structures seen in Figs. 3(a) to 3(f). This deviation from the scaling does not feature in Fig. 9 (which plots the average distance from the edge of chaos vs Reynolds number), as there are few points on the edge which have a large distance from the laminar attractor. (See the histogram in Fig. 1.)

stable, i.e., all infinitesimal perturbations would decay. To find the minimum perturbation we have investigated the edge of chaos separating the laminar state from the turbulent ones. Our method does not employ an optimization procedure as opposed to the "minimal seed" method [35]. On examining Reynolds numbers from 200 to 2000, we find that the nearest point on the edge of chaos to the laminar attractor (and thus the critical amplitude of the perturbation beyond which the laminar attractor becomes unstable), has a distance proportional to $\approx \mathrm{Re}^{-2}$ (Fig. 8). Thus, the critical amplitude of perturbation A_c that can be added to the laminar attractor beyond which the laminar attractor would fall into the turbulent region scales as $A_c \sim \mathrm{Re}^{\alpha}$, with $\alpha = -2$ for the sinusoidal shear flow. This scaling for the sinusoidal shear flow is different compared to the scalings found numerically or experimentally for other flows.

Reference [3] studies a 19-dimensional Galerkin approximation to a parallel shear flow. They choose a fixed initial flow field with a random selection of amplitudes in the 19-dimensional space, scale it up by an amplitude parameter, and plot the lifetimes as a function of amplitude and Reynolds number. They suggest that the critical amplitude scales as Re^{-1}. References [34,41] measure the minimum perturbation for plane Couette flow in terms of the minimum energy needed to destabilize the laminar state. This minimal energy has been found to scale with the Reynolds number as $\sim \mathrm{Re}^{-2}$ in [34] and $\sim \mathrm{Re}^{-2.7}$ in [41]. This minimum energy is, in general, proportional to the square of the minimum distance. Reference [52] predicts an exponent of -1 for plane Couette flow and -1.5 for plane Poiseuille flow. Reference [53] studies experimentally the plane Poiseuille flow and estimates an exponent of -1.5. Reference [54] computes an exponent of -1 for plane Couette flow using direct numerical simulation based on a disturbance in the form of a pair of streamwise vortices. Reference [55] finds numerically that the threshold vortex amplitude to induce instability scales as $\mathrm{Re}^{-1.6}$ in the plane Poiseuille flow and as Re^{-1} in the plane Couette flow.

Various exponents corresponding to the critical amplitude have been suggested for the pipe flow. Reference [42] studies a minimal numerical three-dimensional model of a pipe flow and computes an exponent of -1.5. Reference [43] studies a numerical model of the pipe flow considering streamwise perturbations and finds a dependence of the critical amplitude on the type of perturbation with exponents ranging from -1 to -1.5. Reference [9] carries out numerical simulations of pipe flow using a model with about 1.2×10^5 degrees of freedom and tracks the edge of chaos, computing an exponent of -1. Reference [56] conducts numerical simulations of the pipe flow for autonomous and impulsive forcing scenarios and shows a dependence of the exponent on the type of perturbation and computes exponents ranging from -1 to -1.5. Reference [45] conducts an experimental investigation of a pipe flow and reports that the critical amplitude scales as Re^{-1}. Reference [47] agrees with the results in [45] and also conducts an experimental investigation of a pipe flow for push-pull disturbances computing scaling exponents between -1.3 and -1.5. Reference [57] carries out an experimental investigation of a pipe flow and shows that the edge of chaos is a complicated structure with folds.

Based on our computations for the sinusoidal shear flow, the average distance of the laminar attractor to the edge of chaos scales like $\approx \mathrm{Re}^{-1.8}$ (Fig. 9) and the maximum distance of the laminar attractor to the edge of chaos scales like $\approx \mathrm{Re}^{-1.23}$ (Fig. 10).

We find that the distance of the periodic orbit on the edge from the laminar attractor scales as $\approx \mathrm{Re}^{-1}$ (Fig. 2). Reference [58] investigates a pipe flow and shows that the energy of the saddle state on the edge decreases with Reynolds number, although it does not report an exponent. According to [26], which studies the same system as we study, the average (fluctuation) energy of the periodic orbit on the edge scales as Re^{-2}. Since the energy is given by $E = (1 - a_1)^2 + \sum_{j=2}^{9} {a_j}^2$, the average distance of the periodic orbit on the edge from the laminar attractor would scale as Re^{-1}, which agrees with our computations. We find that the edge of chaos is a stable manifold of a periodic saddle orbit. This is in line with the observation in [26], which investigates the same system, and also with [7], which studies a nine-dimensional system of the plane Couette flow. Reference [26] calculates the probability that an initial condition with a given energy will lead to chaotic behavior by choosing uniformly distributed initial conditions and shows that the periodic orbit on the edge lies in the region corresponding to the energy with 96%–97% probability of transient chaos. This indicates that the distance of the periodic orbit on the edge from the laminar attractor is significantly higher than the average edge distance from the laminar attractor, which agrees with the equations in Figs. 2 and 9.

For Re = 200, 300, 600, 700, 800, 900, 1000, 1500, 2000, we observe an exponential scaling of lifetimes in agreement with the suggestion that the turbulent state represents a chaotic saddle [7,8,10–12,59]. Turbulent bursts in the transient turbulence region persist for an average lifetime

of $\approx \mathrm{Re}^{4.51}$ (Fig. 4). Thus, the average lifetime increases rapidly with Reynolds number but it does not appear that the lifetime would diverge for higher Reynolds numbers. This is in line with the observations in [2,20–22].

Our study covers an interval of Reynolds numbers $200 \leqslant \mathrm{Re} \leqslant 2000$. As the Reynolds number increases, we expect more modes to become active and so higher-dimensional approximations would be more appropriate.

[1] P. G. Drazin and W. H. Reid, *Hydrodynamic Stability* (Cambridge University Press, Cambridge, UK, 1981).
[2] J. Moehlis, H. Faisst, and B. Eckhardt, New J. Phys. **6**, 56 (2004).
[3] B. Eckhardt and A. Mersmann, Phys. Rev. E **60**, 509 (1999).
[4] A. Schmiegel, Transition to Turbulence in Linearly Stable Shear Flows, Ph.D. dissertation, Philipps-Universitat Marburg, Marburg, Germany, 1999.
[5] J. Moehlis, T. Smith, P. Holmes, and H. Faisst, Phys. Fluids **14**, 2493 (2002).
[6] O. Dauchot and N. Vioujard, Eur. Phys. J. B **14**, 377 (2000).
[7] J. D. Skufca, Understanding the Chaotic Saddle with Focus on a 9-variable Model of Planar Couette Flow, Ph.D. dissertation, University of Maryland, College Park, MD, 2005.
[8] J. D. Skufca, J. A. Yorke, and B. Eckhardt, Phys. Rev. Lett. **96**, 174101 (2006).
[9] T. M. Schneider, B. Eckardt, and J. A. Yorke, Phys. Rev. Lett. **99**, 034502 (2007).
[10] B. Eckhardt and H. Faisst, Dynamical systems and transition to turbulence, in *IUTAM Symposium on Laminar-Turbulent Transition and Finite Amplitude Solutions*, edited by T. Mullin and R. R. Kerswell, Fluid Mechanics and its Applications Vol. 77 (Springer, Berlin, 2005), pp. 35–50.
[11] H. Faisst and B. Eckhardt, J. Fluid. Mech. **504**, 343 (2004).
[12] S. Bottin and H. Chate, Eur. Phys. J. B. **6**, 143 (1998).
[13] S. Bottin, F. Daviaud, P. Manneville, and O. Dauchot, Europhys. Lett. **43**, 171 (1998).
[14] T. Mullin and J. Peixinho, J. Low Temp. Phys. **145**, 75 (2006).
[15] J. Peixinho and T. Mullin, Phys. Rev. Lett. **96**, 094501 (2006).
[16] A. P. Willis and R. R. Kerswell, Phys. Rev. Lett. **98**, 014501 (2007).
[17] B. Eckhardt, T. M. Schneider, B. Hof, and J. Westerweel, Annu. Rev. Fluid Mech. **39**, 447 (2007).
[18] T. Mullin and J. Peixinho, Recent observations in the transition to turbulence in a pipe, in *IUTAM Symposium on Laminar-Turbulent Transition*, edited by R. Govindarajan (Springer, Bangalore, 2006), pp. 45–55.
[19] C. Grebogi, E. Ott, and J. A. Yorke, Phys. D **7**, 181 (1983).
[20] B. Hof, J. Westerweel, T. M. Schneider, and B. Eckhardt, Nature (London) **443**, 59 (2006).
[21] T. M. Schneider, State Space Properties of Transitional Pipe Flow, Ph.D. dissertation, Philipps University at Marburg, Marburg, Germany, 2007.
[22] B. Hof, A. de Lozar, D. J. Kuik, and J. Westerweel, Phys. Rev. Lett. **101**, 214501 (2008).
[23] M. Avila, A. P. Willis, and B. Hof, J. Fluid Mech. **646**, 127 (2010).
[24] K. Avila, D. Moxey, A. de Lozar, M. Avila, D. Barkley, and B. Hof, Science **333**, 192 (2011).
[25] J. Moehlis, H. Faisst, and B. Eckhardt, SIAM J. Appl. Dyn. Syst. **4**(2), 352 (2005).
[26] L. Kim and J. Moehlis, Phys. Rev. E **78**, 036315 (2008).
[27] F. Waleffe, Phys. Fluids **9**, 883 (1997).
[28] T. M. Schneider and B. Eckhardt, Chaos **16**, 041103 (2006).
[29] N. R. Lebovitz, Nonlinearity **22**, 2645 (2009).
[30] N. R. Lebovitz, Commun. Nonlinear Sci. Numer. Simul. **17**, 2095 (2012).
[31] N. R. Lebovitz and G. Mariotti, J. Fluid Mech. **721**, 386 (2013).
[32] M. Chantry and T. M. Schneider, J. Fluid Mech. **747**, 506 (2014).
[33] S. Cherubini and P. D. Palma, Fluid Dyn. Res. **46**, 041403 (2014).
[34] Y. Duguet, L. Brandt, and B. R. J. Larsson, Phys. Rev. E **82**, 026316 (2010).
[35] R. R. Kerswell, C. C. T. Pringle, and A. P. Willis, Rep. Prog. Phys. **77**, 085901 (2014).
[36] C. C. T. Pringle and R. R. Kerswell, Phys. Rev. Lett. **105**, 154502 (2010).
[37] C. C. T. Pringle, A. Willis, and R. Kerswell, J. Fluid Mech. **702**, 415 (2012).
[38] A. Monokrousos, A. Bottaro, L. Brandt, A. Di Vita, and D. S. Henningson, Phys. Rev. Lett. **106**, 134502 (2011).
[39] S. M. E. Rabin, C. P. Caulfield, and R. R. Kerswell, J. Fluid Mech. **712**, 244 (2012).
[40] S. Cherubini and P. D. Palma, J. Fluid Mech. **716**, 251 (2013).
[41] Y. Duguet, A. Monokrousos, L. Brandt, and D. Henningson, Phys. Fluids **25**, 084103 (2013).
[42] A. P. Willis and R. R. Kerswell, J. Fluid Mech. **619**, 213 (2009).
[43] F. Mellibovsky and A. Meseguer, Phys. Fluids **18**, 074104 (2006).
[44] H. Shan, Z. Zhang, and F. T. M. Nieuwstadt, Int. J. Heat Fluid Flow **19**, 320 (1998).
[45] B. Hof, A. Juel, and T. Mullin, Phys. Rev. Lett. **91**, 244502 (2003).
[46] B. Hof, Transition to turbulence in pipe flow, in *Laminar-Turbulent Transition and Finite Amplitude Solutions*, edited by T. Mullin and R. R. Kerswell (Springer, Berlin, 2004), pp. 221–231.
[47] J. Peixinho and T. Mullin, J. Fluid Mech. **582**, 169 (2007).
[48] See Supplemental Material at http://link.aps.org/supplemental/10.1103/PhysRevE.91.052903 for model analyzed in the paper.
[49] H. E. Nusse and J. A. Yorke, Phys. D **36**, 137 (1989).
[50] T. Kreilos and B. Eckhardt, Chaos **22**, 047505 (2012).
[51] T. Kreilos, B. Eckhardt, and T. M. Schneider, Phys. Rev. Lett. **112**, 044503 (2014).
[52] S. J. Chapman, J. Fluid Mech. **451**, 35 (2002).
[53] J. Philip, A. Svizher, and J. Cohen, Phys. Rev. Lett. **98**, 154502 (2007).

[54] G. Kreiss, A. Lundbladh, and D. S. Henningson, J. Fluid Mech. **270**, 175 (1994).
[55] S. C. Reddy, P. J. Schmid, J. S. Baggett, and D. S. Henningson, J. Fluid Mech. **365**, 269 (1998).
[56] F. Mellibovsky and A. Meseguer, Philos. Trans. A. Math. Phys. Eng. Sci. **367**(1888), 545 (2009).
[57] Y. Tasaka, T. M. Schneider, and T. Mullin, Phys. Rev. Lett. **105**, 174502 (2010).
[58] T. M. Schneider and B. Eckhardt, Philos. Trans. R. Soc. A **367**, 577 (2009).
[59] J. Vollmer, T. Schneider, and B. Eckhardt, New J. Phys. **11**, 013040 (2009).